Materiales de Construcción
Vol. 72, Issue 346, April-June 2022, e285
ISSN-L: 0465-2746
https://doi.org/10.3989/mc.2022.15821

Long-term efficiency of silica fume and fly ash to suppress ASR in field structures

A. Leemann[a] ✉, C. Merz[b]

a. Empa, Swiss Federal Laboratories for Materials Science and Technology, Concrete and Asphalt Laboratory, (Dübendorf, Switzerland)
b. Merz Ingenieurberatung, (Möriken, Switzerland)
✉: andreas.leemann@empa.ch

Received 26 October 2021
Accepted 10 February 2022
Available on line 25 April 2022

ABSTRACT: The potential of ASR in concrete can be assessed by the concrete prism test. However, the transferability of the results obtained with accelerated tests to concrete behavior under field conditions has to be validated. Such a validation was performed ten years ago for concrete produced with Portland cement and various Swiss aggregates. In recent years, the use of supplementary cementitious materials (SCM) has increased. So far, no validation for such types of concrete has been conducted in Switzerland. The goal of the current project is to fill this gap and provide the missing validation. Eight structures where chosen for the investigation. In all of them concrete containing SCM was used and the results of the concrete prism test at time of construction were available. In general, the results of the concrete prism test correlate with the degree of damage in the structures assessed by the analysis of the microstructure.

KEY WORDS: Alkali-aggregate reaction; Concrete prism test; Field exposure; Validation; Microstructure.

Citation/Citar como: Leemann, A.; Merz, C. (2022) Long-term efficiency of silica fume and fly ash to suppress ASR in field structures. Mater. Construcc. 72 [346], e285. https://doi.org/10.3989/mc.2022.15821.

RESUMEN: *Eficiencia a largo plazo del humo de sílice y de las cenizas volantes para evitar la reacción álcali-sílice en estructuras reales*. La reactividad potencial álcali-sílice (RAS) en el hormigón puede evaluarse mediante ensayos de prismas de hormigón. Sin embargo, debe validarse la transferencia de los resultados obtenidos mediante ensayos acelerados con el comportamiento del hormigón en condiciones reales. El ensayo acelerado de prismas de hormigón se realizó hace diez años para distintos hormigones fabricados con cemento Portland y diferentes áridos suizos. En los últimos años se ha incrementado el uso de adiciones. Hasta ahora, no se había realizado ninguna validación de estos hormigones en Suiza. El objetivo de este trabajo es llenar este vacío y proporcionar la validación que falta. Se eligieron ocho estructuras para la investigación. En todos los casos se había utilizado hormigón con adiciones y se disponía del ensayo de prismas de hormigón en el momento de la construcción. En general, los resultados de estos ensayos se correlacionan con el grado de daño en las estructuras, evaluándolas mediante análisis microestructural.

PALABRAS CLAVE: Reacción árido-álcali; Ensayo de prismas de hormigón; Exposición real; Validación; Microestructura.

This article was selected among the papers presented at the 2022 *International Conference on Alkali-Aggregate Reaction in Concrete* (16th ICAAR)

1. INTRODUCTION

The concrete prism test (CPT) is one approach used to assess the potential for an alkali-silica reaction (ASR) of a given mix design. As such, it is an important tool in designing concrete resistant to ASR. However, the transferability of the results obtained with accelerated tests to concrete behaviour under field conditions has to be validated. A validation of the Swiss CPT and the transferability of its results to concrete structures have been established in (1). However, only concrete produced with Portland cement (CEM I) was used in this validation. Supplementary cementitious materials (SCM) are increasingly used for concrete production either to reduce cement clinker content and with it CO_2 emissions or as a way to mitigate ASR. Nowadays, blended cements dominate the Swiss cement market. So far, the transferability of the results of the CPT to concrete in field conditions has not been validated for mix designs containing SCM in Switzerland. Internationally, some information is provided by current field exposure sites where concrete blocks produced in the laboratory are stored outdoors. Their expansion is surveyed and compared to results of the CPT (2-6). However, these studies cover only the behaviour of the specific aggregate-binder combinations used. As every reactive aggregate exhibits a characteristic behaviour in regard to expansion and as the cement composition and its effect on ASR can vary substantially, a validation of the CPT with Swiss materials is mandatory for a validation. Therefore, a project using a similar approach as in (1) was started. Structures were identified where two prerequisites were present. Firstly, the concrete mix design had to include reactive aggregates, fly ash (FA), silica fume (SF) or a combination of both SCM. Secondly, results of the CPT conducted at the time of construction had to be available. Eight structures fulfilling the criteria described above were identified. The goal of the project was to verify:

- whether FA and SF have the same effect on ASR in the CPT on the short term and on the structures on the long term;
- whether the expansion reached in the CPT shows a relation to eventual damages observed in the structures.

The selected structures were inspected, coring sites were defined and several cores were extracted. The concrete was analyzed using optical microscopy (OM) and scanning electron microscopy (SEM) with energy-dispersive X-ray spectroscopy (EDX). Then the determined degree of damage was compared to the expansion obtained in the CPT. More detailed results than presented here are available in (7).

2. MATERIALS AND METHODS

2.1. Materials

All investigated structures were built between 1999 and 2007, translating to an age of 11 to 17 years when this analysis was performed. Information about the structure type, age and location, the used concrete mix design, the alkali content of the concrete, the results of the CPT and reactivity of the aggregates are given in Table 1. All accelerated ASR tests were conducted once for each structure before construction. Consequently, cement, SCM and aggregates for the CPT were not from the same batch as used for the structures but from the same plants and quarries, respectively. Additionally, the mix designs in the CPT and the corresponding structures were identical.

The aggregates were tested with the ultra-accelerated microbar test according to AFNOR XP 18-594 (four prisms: 10 x 10 x 40 mm^3 (8)). The limit value of expansion to identify potentially reactive aggregates is 0.11 %. Consequently, all aggregates used for the investigated structures were classified as potentially reactive (Table 1).

The CPT as used nowadays in Switzerland (9) was not standardized before 2012. Therefore, there were some variations in the CPT protocol used for the concrete mixtures in the early 2000's. All the concrete mixtures except one (the viaduct in Dangelstutz BE) were boosted with NaOH corresponding to 25 mass-% of the total alkali content of the concrete. The specimens (three prisms: 70 x 70 x 280 mm^3) were stored in a reactor at a temperature of 60 °C and close to 100 % relative humidity. Test duration varied between 5 and 18 months. In the early 2000's, a general limit value of 0.2 ‰ was applied to distinguish between ASR resistant concrete mixtures and non ASR-resistant concrete mixtures. In spite of the fact that two concrete mixtures expanded more than 0.2 ‰, they were still used for construction. In the current standard (1), the limit values of expansion after 5 months and after 12 months are 0.2 and 0.3 ‰, respectively.

After defining coring sites, cores with a diameter of 50 mm and varying length were extracted. Samples for the production of thin sections were selected, cut, dried in the oven at 50 °C for three days and epoxy impregnated. Then thin section measuring 50 × 90 mm^2 were produced. The samples to be studied in the SEM were prepared in the same way as the samples for thin sections. After epoxy impregnation, disc-shaped, polished samples with a diameter of 50 mm were produced and carbon coated for SEM analysis.

2.2. Methods

The state of the structures was assessed by visual inspection. Narrow cracks (< 0.5 mm) were usually present on the concrete surface of the investigated structures. However, the extent of cracking was too low for the determination of a meaningful crack-index.

2-4 thin sections (50 × 90 mm^2) per structure were studied using a Zeiss Axioplan polarisation microscope. The crack-index was determined using the ap-

Table 1. Investigated structures with concrete mix design, alkali content (without boosting) determined on the materials used for the CPT and expansion determined using the Swiss CPT and the microbar test. All concrete mixtures tested with the CPT were boosted with an amount of NaOH representing 25 mass-% of the total alkali content of the concrete (third row) except in the case of the viaduct. w/c_{eq} uses K-factor for FA of 0.4 and for MS of 1.0.

Type of structure Year of construction	Concrete mix design	Alkali-content of concrete [kg Na_2Oeq/m^3]	Expansion CPT	Origin of aggregate Expansion microbar test
River dam (Wettingen (AG), 1930-1933, repair 2005-2007)	CEM I 340 kg/m³ FA 50 kg/m³ SF 20 kg/m³ w/c_{eq} = 0.45	3.1 kg/m³	-0.003 ‰ after 8 month	Alluvial gravel Middleland 2.35 ‰
Viaduct (Dangelstutz (BE), 1999-2000)	CEM II/A-LL 305 kg/m³ FA 20 kg/m³ w/c_{eq} = 0.49	2.3 kg/m³	0.049 ‰ after 5 month[3]	Gravel of Bernese Alps 1.97 ‰
Bridge 1 (Fully (VS), 2004-2006)	CEM I 300 kg/m³ FA 100 kg/m³ w/c_{eq} = 0.42	2.6 kg/m³	0.122 ‰ after 5 month	Alluvial gravel of Rhone valley 2.50 ‰
Oil-water basin (Vevey (VD), 2005)	CEM I (with 4 mass-% SF) 350 kg/m³ FA 50 kg/m³ w/c_{eq} = 0.46	3.0 kg/m³	0.161 ‰ after 12 month	Alluvial gravel of Rhone valley 1.89 ‰
Various components of Subway (Lausanne (VD), 2004-2007)	CEM I 350 kg/m³ FA 25 kg/m³ w/c_{eq} = 0.46	3.2 kg/m³	0.171 ‰ after 5 month	Alluvial gravel of Middleland 0.95 und 1.61 ‰
Bridge 2 (Visp (VS), 2004-2006)	CEM I 325 kg/m³ SF 20 kg/m³ w/c_{eq} = 0.45	2.6 kg/m³	0.259 ‰ after 18 month	Alluvial gravel of Vispa No data
Train station (Salgesch (VS), 2004	CEM I 270 kg/m³ FA 80 kg/m³ w/c_{eq} = 0.48	2.6 kg/m³	0.265 ‰ after 5 month	Alluvial gravel of Rhone valley 1.79 ‰
Tunnel entrance (Collombey (VS), 2003	CEM I ca. 350 kg/m³ SF + FA < 50 kg/m³ w/c_{eq} ca. 0.44	3.1 kg/m³	0.300 ‰ after 5 month	Alluvial gravel of Rhone valley 2.04 ‰

proach described in (10), taking into account micro cracks ≥ 5 µm. 2-8 thin sections were studied per structure by optical microscopy.

The polished samples were studied using a FEI Quanta 650 applying a pressure between 3.0 and 4.0×10^{-6} Torr. Chemical analysis was performed by EDS with a Thermo Noran Ultra Dry 60 mm² detector and Pathfinder X-Ray Microanalysis Software. An acceleration voltage of 12.0 kV and a spot size of 4.5 was used for imaging and EDS analysis. The images were acquired in the backscattering mode. Two disc-shaped polished sections with a diameter of 50 mm were studied per coring site. Element ratios are given based on atomic-%.

3. RESULTS

3.1 River dam

The presence of FA and SF and the type of cement used are confirmed (nominal binder composition: cement (CEM I (340 kg/m³), FA (50 kg/m³) and SF (20 kg/m³). The aggregates represent the typical material used in the Swiss Middleland, consisting of alluvial deposits of well-rounded carbonate and silicate rocks originating from the Alps.

The FA particles are easily identified. SF was poorly dispersed and forms a lot of agglomerates up to a diameter of 0.4 mm, displaying crack formation (Figure 1A). The high Ca/Si-ratio in the interior of the aggregate indicates that it has fully reacted and has no expansion potential left (Figure 1B).

Some of the cracks display the typical characteristics of early age shrinkage, propagating around aggregate particles instead of through them. At a depth > 4 cm, the cracks start to run through the aggregates. Some of them display ettringite. Ettringite is present as well in many air voids.

The total crack-index is 0.53 mm/m; without taking into account cracks < 5 µm it is 0.15 mm/m.

ASR products in the aggregates are nearly absent. Only in one aggregate, a thin crack lining, albeit too narrow for accurate EDS analysis, was present.

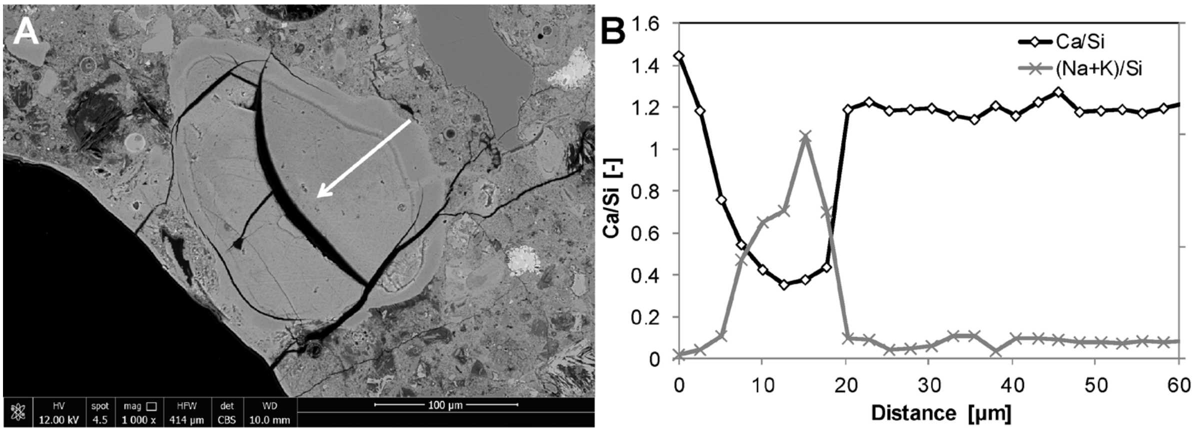

Figure 1. (A) SF agglomerate. The white arrow indicates location and direction of the EDS line scan shown in (B). Horizontal field width (HFW) = 414 µm. (B) Ca/Si- and (Na+K)/Si-ratio close to the edge of a SF agglomerate displaying a zone with decreased Ca/Si-ratio and high Na/K-ratio close to the surface. River dam.

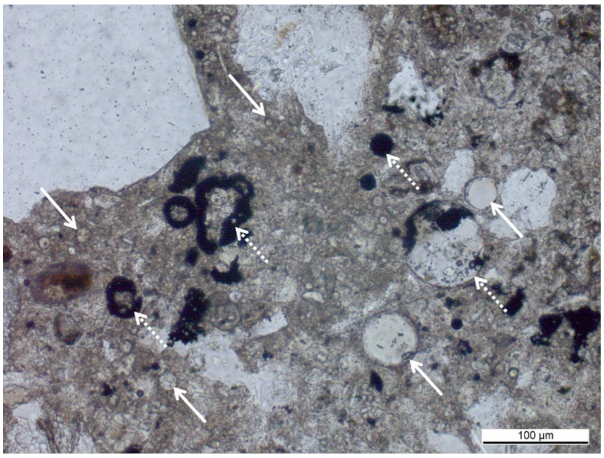

Figure 2. Relatively large iron-bearing (dotted white arrows) and small FA particles without iron (white arrows) in the cement paste. Thin section in polarized light. Bridge 1.

3.2. Viaduct

The type of cement used and the presence of a minor amount of FA are confirmed (nominal binder composition: CEM II/A-LL 305 kg/m^3, FA 20 kg/m^3). The well-rounded aggregates are composed of granite and siliceous sandstone with minor amounts of limestone and gneiss. There are numerous microcracks in the aggregates, mainly concentrating on granite and gneiss. Usually, these microcracks do not extend into the cement paste and it is likely that these cracks were already present before the aggregates were used for concrete production However, in a few cases cracks extend from sandstone aggregates into the cement paste. In some of these cracks, crystalline ASR products are present as partial fillings. Only in one case, a completely filled crack is observed. The crack-index is 0.46 mm/m.

3.3. Bridge 1

The presence of a major amount of FA (Figure 2) and the use of CEM I are confirmed (nominal binder composition: CEM I 300 kg/m^3, FA 100 kg/m^3). Gneiss and schists are the major components of the aggregates with about 30 % carbonates. Microcrystalline quartz as a typical reactive mineral is present both in gneiss and schist.

Typical ASR-related cracks extending from the aggregates into the cement paste are only marginally present. No ASR products in the aggregates are detectable in the thin sections. In the SEM, minor amounts of crystalline ASR products can be observed.

3.4. Oil-water basin

Cement type and FA as mineral addition are confirmed (nominal binder composition: CEM I containing 4 mass-% of SF as minor constituent 350 kg/m^3, FA 50 kg/m^3). Some silica agglomerates with a diameter of up to 30 µm are present. The aggregates contain limestone, limestone with detritic silicates, quartzite, sandstone, gneiss and schist. The particles range from well-rounded to crushed.

The aggregates display numerous microcracks that often extend into the cement paste. No ASR can optically be identified in the thin sections.

In the majority of the aggregates, ASR products are observed in the SEM. They mostly occur as isolated bundles but can fill cracks entirely in a few cases (Figure 3).

The determination of the crack-index resulted in a value of 0.30 mm/m.

3.5. Subway

Cores from three structures, all part of the subway line, were studied. The same concrete mix

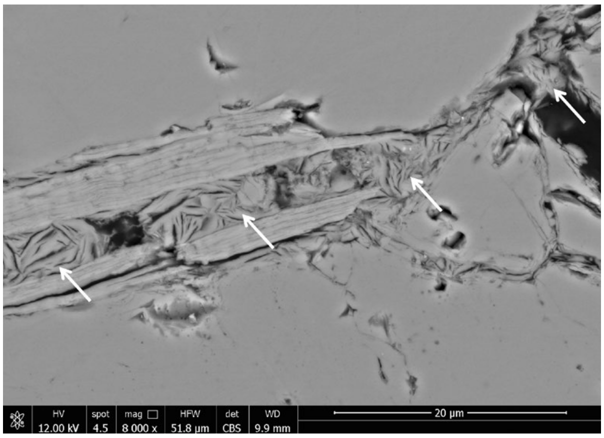

FIGURE 3. Crack in gneiss particle filled with crystalline ASR products (white arrows). Oil-water basin. HFW = 52 µm.

design was used in all three of them. The minor amount of FA and the cement type are confirmed (nominal binder composition: CEM I 350 kg/m^3, FA 25 kg/m^3). Limestone (70 %) with a minor amount of siliceous inclusions and sandstone (30 %) with minor amounts of silicates compose the well-rounded aggregate. A relatively alkali-reactive filler (crushed siliceous sandstones) was added to the concrete.

Two of the three structures do not show any signs of ASR. Both of them are not exposed to the weather and are not in contact with bedrock. However, in the third one, a supporting wall exposed to precipitation, clear signs of ASR are present. They manifest as microcracks extending from the aggregates into the cement paste. While the resolution of the optical microscope does not allow the identification of ASR products, they are identifiable in the SEM as partial crack fillings in limestones containing siliceous inclusions and in silicates.

The crack-index is 0.52 mm/m in the ASR-affected supporting wall.

3.6. Bridge 2

The cement type and SF occasionally forming agglomerates < 20 µm are confirmed (nominal binder composition: CEM I 325 kg/m^3, SF 20 kg/m^3). The well-rounded aggregates mainly consist of gneiss and schist with traces of carbonate particles (~ 5 %).

There are numerous aggregates displaying microcracks extending into the cement paste. No ASR products can be observed in the thin sections. SEM reveals that crystalline ASR products are present as partial crack fillings.

A value of 0.42 mm/m was determined for the crack-index.

3.7. Railway station

The use of a substantial amount of FA and the cement type are confirmed (nominal binder composition: CEM I 270 kg/m^3, FA 80 kg/m^3). The crushed aggregate consist of gneiss and schist with some carbonates corresponding to about 20 %.

Numerous aggregate particles exhibit ASR-typical cracks running from the aggregates into the cement paste. The cracks form an interconnected network comprising the entire concrete. However, no ASR products are recognizable by optical microscopy. In the majority of the affected aggregates, ASR products are identifiable with SEM as partial crack fillings (Figure 4). The crack-index is 0.43 mm/m.

3.8. Tunnel entrance

The cement type and minor amounts of FA and SF, the latter with some agglomerates < 30 µm, are confirmed (nominal binder composition: CEM

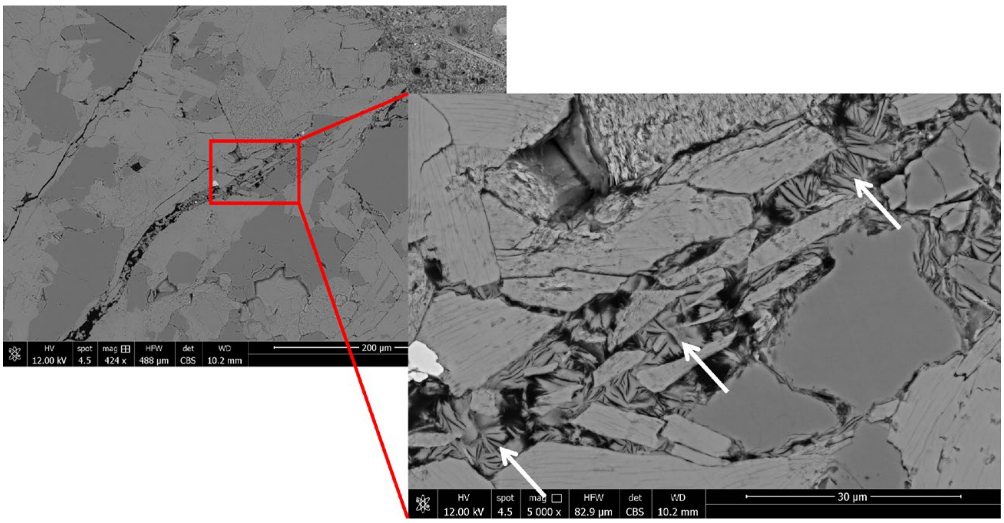

FIGURE 4. Crack in gneiss particle partially filled with crystalline ASR products (white arrows). Railway station. HFW = 424 µm (left) and 83 µm (right).

I 300-350 kg/m^3, FA 20-40 kg/m^3, SF 10 kg/m^3). A mixture of silicate and carbonate rocks (~30 %) were used as aggregates.

Only about 5% of the aggregates display cracks running from the aggregates into the cement paste. In a few of these aggregates, ASR products can be observed by optical microscopy. Additionally, there are ASR products in air voids located in the cement paste. With the SEM, all crack-affected aggregates show partial or complete crack fillings.

The determination of the crack-index reveals a value of 0.48 mm/m.

3.9. Composition of ASR products

The crystalline ASR products present in aggregates consist of silicon as the main components and additionally potassium, sodium and calcium showing only little variation in the different structures (Figure 5). Only the products formed in aggregates of bridge 1 contain slightly less alkalis and calcium compared to the other ones. The Na/K-ratio ranges from 0.20 to 0.48. These values may be influenced by releasable alkalis of some aggregates or the alkalis present in the used FA, both potentially affecting the Na/K-ratio. These values are in agreement with results reported in (1, 11-13).

4. DISCUSSION

At the time of the investigation, the structures were still relatively recent for the development of ASR, since Swiss aggregates are known for their slow reaction. Still, the microstructural features present permit to assess the state of damage, the stage of ASR and with it an approximate assessment of its future development.

ASR present in the River dam is not caused by the aggregates, but by the poorly dispersed SF forming large agglomerates. The microstructure clearly indicates that these agglomerates have been expanding, leading to ASR-typical cracks. In the CPT the concrete showed no expansion at all. It can be assumed that the SF used to produce the concrete prism for the accelerated test was well dispersed, mitigating ASR instead of triggering it.

The expansion in the CPT in case of the viaduct was very low with a value of 0.05 ‰. This seems to be in contrast to the clear signs of ASR present in the structure. However, it has to be taken into account that no alkali boosting was used for the CPT in this particular case. With alkali boosting the expansion in the CPT might have been higher. This would have placed the expansion value more in line with the damage observed in the structure.

The few signs of ASR in bridge 1 go well together with the expansion in the CPT that is clearly below the limit value of 0.2 ‰. The used dosage of FA (100 kg/m^3) was probably effective to suppress ASR in spite of the highly reactive aggregate.

The expansion potential of the concrete used for the oil-water basin is indicated as low by the CPT with a value of 0.13 ‰ after five months. On the other hand, the microstructural analysis indicates a moderate damage. In this case, the CPT somewhat underestimates the ASR potential.

The three studied structures of the subway clearly show the effect of exposure. Only the structure exposed to rain showed ASR in spite of the identical mix design in all three structures. The expansion in the CPT that is slightly below the limit value seems to go along with the ASR status of the affected structure.

The CPT of the concrete used in bridge 2 resulted in an expansion just below the limit value. Therefore, the assessed damage and damage potential assessed by the microstructural investigation fit well.

The microstructure of the concrete used in the Railway station shows that the majority of the aggregates is affected by ASR leading to a connected

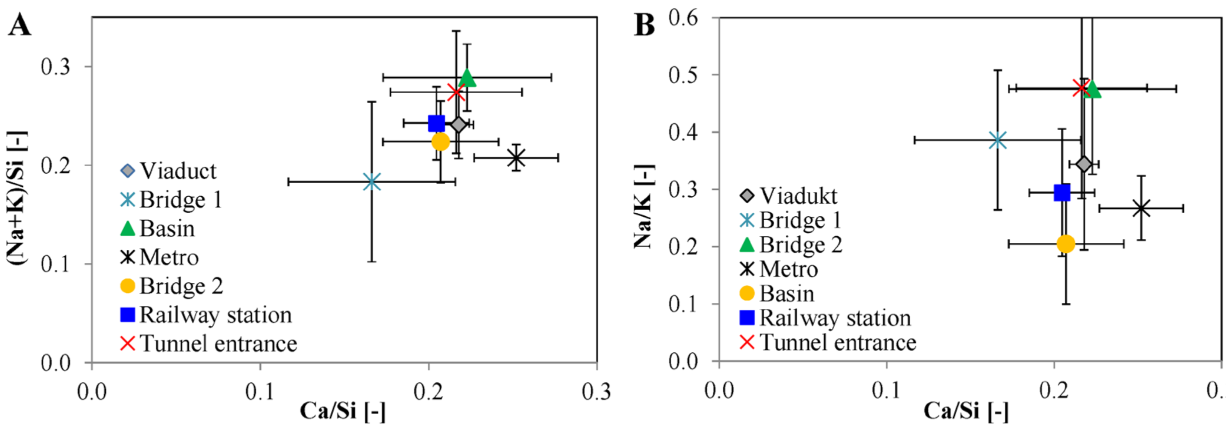

FIGURE 5. (Na+K)/Si-ratio (A) and Na/K-ratio (B) as a function of the Ca/Si-ratio of the crystalline ASR products formed in the aggregates of the different structures.

network of microcracks. This seems to be no surprise because the structure is exposed to the weather and the CPT clearly indicated a potentially reactive concrete with an expansion above the limit value.

The tunnel entrance showed the most developed ASR of the studied structures, with relatively few affected aggregates but the formation of ASR products already easily observable with the optical microscope. Here again, this was to be expected as the CPT indicated a potentially reactive concrete with an expansion of 0.3 ‰.

The comparison between the expansion potential in the CPT and the observed damage in the microstructural analysis are summarized in Figure 6. As the structures are relatively recent and ASR is in its early stage, the values for the crack-index are low. Still, there is a trend for an increased crack-index with increasing expansion in the CPT. The only outlier is the viaduct. As already explained above, this is likely the result of the missing alkali boosting in the CPT. With alkali boosting, the expansion of the CPT in case of the viaduct would have moved into the direction of the arrow in Figure 6. The viaduct is not taken into account in the calculation of the regression line. Additionally, the value of the river dam is not shown, because SF agglomerates were responsible for expansion and not the aggregates. A qualitative assessment in regard to the expansion potential of the structures in the future based on age and crack index is shown in Table 2.

The used dosages of SCM were only able to suppress ASR nearly completely in the case of bridge 1. In the other cases, ASR was only slowed down. The observed damages were clearly lower than in other structures produced with concrete containing the same or similar aggregates and no SCM. However, it seems to be advisable to use at least 100 kg/m^3 of FA to suppress ASR with the type of aggregates used. In the case of bridge 2 even a dosage of 20 kg/m^3 of SF was not sufficient to eliminate ASR. Additionally, the combination of relatively low doses of FA and SF has not been shown to be fully effective.

In regard to the microstructural analysis, thin sections are well suited to identify expanding aggregate

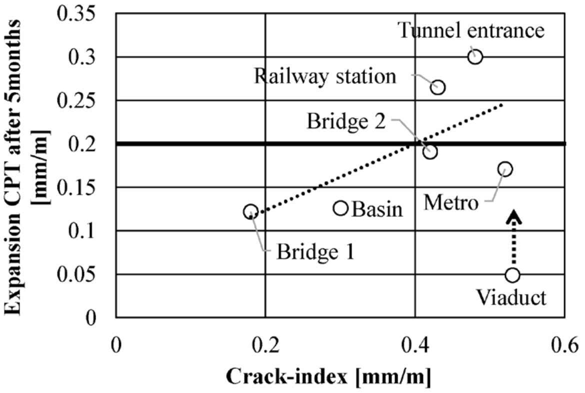

Figure 6. Expansion in the CPT as a function of crack-index.

particles based on the crack patterns, to determine a crack-index and to identify larger deposits of ASR products formed in aggregates and extrusions thereof into the cement paste. However, often the small amount of crystalline ASR products present in aggregates at an early stage of the reaction are below the resolution limit of optical microscopy. Therefore, the combination of optical microscopy with SEM/EDX is beneficial to verify the presence of ASR without ambiguity.

Table 2. Qualitative assessment of the expansion potential determined with the CPT and degree/damage potential of ASR in the different structures based on their current state.

Structure	AAR expansion potential based on CPT	Assessed ASR damage potential in the future of structure
River dam	very low	very low
Viaduct	low	low to medium
Bridge 1	low	low
Oil-water basin	low	medium
Subway	low to medium, below limit value	medium
Bridge 2	low to medium, below limit value	medium
Train station	medium to high	medium to high
Tunnel entrance	medium to high	high

5. CONCLUSIONS

The expansion of the CPT was compared with the condition of concrete structures in which the same mix design used in the CPT was applied. The different concrete mix design contained both reactive aggregates and SCM. Based on the results, the following conclusions can be drawn:

- The CPT seems to be suitable to asses the expansion potential of concrete containing SCM used in structures. However, the database has to be enlarged for further verification.
- Alkali boosting of the concrete used for the CPT seems to be necessary to better reflect the behaviour of the concrete in the structure.
- Using different batches of SF and likely FA for the CPT and the structure may lead to a change in the expansion potential of one or the other.
- Low amounts of SCM (FA ≤ 80 kg/m^3, SF ≤ 20 kg/m^3), even when used in combination, are not able to prevent ASR and seem only successful in slowing down the reaction.
- The analysis of thin sections is a suitable tool to determine the crack-index and identify

expanding aggregate particles. However, it has to be complemented by SEM with EDX to identify ASR products in an early stage of reaction.

ACKNOWLEDGEMENTS

The authors would like to thank the Federal Roads Office (FEDRO) for financing this study and Pietro Lura for reviewing the manuscript.

AUTHOR CONTRIBUTIONS:

Conceptualization: A. Leemann, C. Merz. Formal analysis: A. Leemann, C. Merz. Funding acquisition: C. Merz. Investigation: A. Leemann, C. Merz. Methodology: A. Leemann, C. Merz. Project administration: C. Merz. Writing - original draft: A. Leemann, C. Merz. Writing - review & editing: A. Leemann.

REFERENCES

1. Leemann, A.; Merz, C. (2013) An attempt to validate the ultra-accelerated microbar and the concrete performance test with the degree of AAR-induced damage observed in concrete structures. *Cem. Concr. Res.* 49, 29-37. https://doi.org/10.1016/j.cemconres.2013.03.014.
2. Thomas, M.; Fournier, B.; Folliard, K.J.; Ideker, J.; Shehata, M. (2006) Test methods for evaluating preventive measures for controlling expansion due to alkali–silica reaction in concrete. *Cem. Concr. Res.* 36 [10], 1842-1856. https://doi.org/10.1016/j.cemconres.2006.01.014.
3. Fournier, B.; Ideker, J.H.; Folliard, K.J.; Thomas, M.D.A.; Nkinamubanzi, P-C.; Chevrier, R. (2009) Effect of environmental conditions on expansion in concrete due to alkali-silica reaction (ASR). *Mater. Charact.* 60 [7], 669-679. https://doi.org/10.1016/j.matchar.2008.12.018.
4. Ideker, J.H.; Drimalas, T.; Bentivegna, A.F.; Folliard, K.J.; Fournier, B.; Thomas, M.D.A.; Hooton, R.D.; Rogers, C.A. (2012) The importance of outdoor exposure site testing. In: Proceedings of the 14th International Conference on Alkali Aggregate Reactions (ICAAR), Austin, Texas.
5. Fournier, B.; Chevrier, R.; Bilodeau, A.; Nkinamubanzi, P.C.; Bouzoubaa, N. (2016) Comparative field and laboratory investigations on the use of supplementary cementing materials (SCMs) to control alkali-silica reaction (ASR) in concrete. In: Proceedings of the 15th International Conference on Alkali Aggregate Reactions (ICAAR), Sao Paolo, Brasil.
6. Wigum, B.J.; Einarsson, G.J. (2016) Alkali aggregate reaction in Iceland: results from laboratory testing compared to field exposure site. In: Proceedings of the 15th International Conference on Alkali Aggregate Reactions (ICAAR), Sao Paolo, Brasil.
7. Merz, C.; Leemann, A. (2019) AAR-Prävention für Beton: Erfahrungen mit Zusatzstoffen, Bericht VSS Nr. 694, Bern.
8. AFNOR XP 18-594 (2004) Méthodes d'essai de reactivité aux alcalis. Association Française de Normalisation, Paris.
9. SN 505 262/1 (2019) Betonbau - Ergänzende Festlegungen. Appendix G. Schweizer Ingenieur- und Architektenverein, Zürich.
10. Leemann, A.; Griffa, M. (2013) Diagnosis of alkali-aggregate reaction in dams, state of the art report, SFOE-Project SI/500863-01, Bern.
11. Thaulow, N.; Jakobsen, U.H.; Clark, B. (1996) Composition of alkali silica gel and ettringite in concrete railroad ties: SEM-EDX and X-ray diffraction analyses. *Cem. Concr. Res.* 26 [2], 309-318. https://doi.org/10.1016/0008-8846(95)00219-7.
12. Katayama, T.; Drimalas T.; Ideker J.H.; Fournier B. (2012) ASR gels and their crystalline phases in concrete - universal products in alkali-silica, alkali-silicate and alkali-carbonate reactions. In Proceedings of the 14th International Conference on Alkali Aggregate Reactions (ICAAR), Austin, Texas (pp. 20-25).
13. Leemann, A.; Shi, Z.; Wyrzykowski, M.; Winnefeld, F. (2020) Moisture stability of crystalline alkali-silica reaction products formed in concrete exposed to natural environment. *Mater. Design.* 195, 109066. https://doi.org/10.1016/j.matdes.2020.109066.